ACS Catalysis

Research Article

pubs.acs.org/acscatalysis

Lewis Acid Catalysis of TiO_4 Tetrahedra on Mesoporous Silica in Water

Hiroshi Shintaku,[†] Kiyotaka Nakajima,[†,‡] Masaaki Kitano,[§] Nobuyuki Ichikuni,[∥] and Michikazu Hara*[,†,¶]

[†]Materials and Structures Laboratory, Tokyo Institute of Technology, 4259-R3-33 Nagatsuta, Midori-ku, Yokohama 226-8503, Japan

[‡]Japan Science and Technology (JST) agency, PRESTO, 4-1-8 Honcho, Kawaguchi 332-0012, Japan

[§]Materials Research Center for Elemental Strategy, Tokyo Institute of Technology, 4259 Nagatsuta, Midori-ku, Yoko-hama 226-8503, Japan

[∥]Department of Applied Chemistry and Biotechnology, Graduate School of Engineering, Chiba University, Inage-ku, Chiba 263-8522, Japan

[¶]Japan Science and Technology (JST) agency, ALCA, 4-1-8 Honcho, Kawaguchi 332-0012, Japan

ABSTRACT: TiO_4-deposited mesoporous silica (TDMS) was studied as a water-tolerant solid Lewis acid catalyst. TDMS prepared by a simple postgrafting technique using Ti(*i*-pro)$_4$ has a large BET surface area (ca. 450 m^2 g^{-1}) and ordered mesoporous structure. Ultraviolet−visible diffuse reflectance spectroscopy (UV−vis DRS), X-ray absorption near edge structure (XANES), and CO adsorption measurements with Fourier transform infrared (FTIR) spectroscopy revealed that isolated TiO_4 tetrahedra on TDMS have Lewis acidity, even in the presence of water. Lewis acid centers on TDMS exhibit higher catalytic performance for the hydride transfer of pyruvaldehyde to lactic acid and the Mukaiyama-aldol condensation of benzaldehyde with 1-trimethylsilyloxy-cyclohexene in water than that of conventional heterogeneous and homogeneous Lewis acids, including scandium(III) triflate (Sc(OTf)$_3$), which also works even in water. The high catalytic performance of TDMS can be attributed to Lewis acid catalysis of isolated TiO_4 tetrahedra in water.

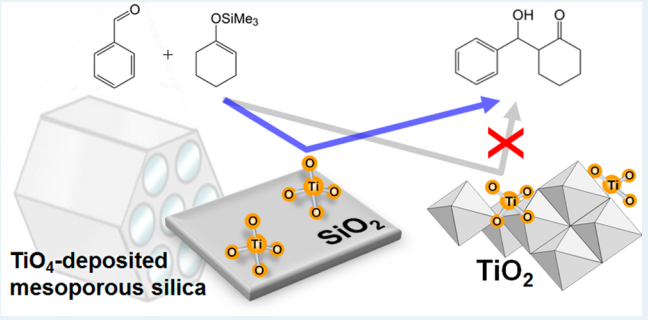

KEYWORDS: *Lactic acid, Lewis acid catalyst, mesoporous silica, Mukaiyama-aldol reaction, titanium tetrahedra*

1. INTRODUCTION

Lewis acids, such as $AlCl_3$ and $TiCl_4$, are essential catalysts for the production of a variety of petroleum-derived chemicals, such as polymers and pharmaceuticals.[1,2] However, the use of conventional Lewis acids require strictly anhydrous conditions because they are decomposed and/or completely deactivated by water. In addition, excess amounts of Lewis acid are often necessary for efficient Lewis acid catalyzed reactions, accompanied with the production of corrosive acid waste by neutralization.[3] Some attempts have been made to develop water-compatible and easily separable solid Lewis acid catalysts to reduce the environmental impact of reaction systems. For example, polymer-supported lanthanide triflates have been studied as heterogeneous Lewis acid catalysts for various water-participating organic reactions, such as aldol condensation and the Diels−Alder reaction, under mild conditions.[4,5] The Sn center on Sn-Beta zeolite can act as a water-tolerant Lewis acid site to promote the Baeyer−Villiger oxidation of ketones with hydrogen peroxide.[6,7] The unique catalysis with Sn-Beta zeolite is attributed not only to the selective activation of hydrogen peroxide but also to the carbonyl group in the reactant; the activated carbonyl group on a Lewis acid site preferentially reacts with hydrogen peroxide to form lactone in the presence of water. Sn-Beta zeolite also effectively catalyzes the hydride transfer of glucose into fructose in water[8,9] and methyl lactate production from 1,3-dihydroxyacetone in methanol.[10] However, the utility of polymer-supported lanthanide triflates and Sn-Beta zeolte have been limited by the scarcity of lanthanide and the narrow reaction spaces of zeolites, respectively.

We have recently reported that some early transition metal oxides, such as Nb_2O_5 and TiO_2, can work in water as insoluble Lewis acid catalysts and are applicable to the conversion of glucose into 5-hydroxymethylfurfural and lactic acid production from pyruvaldehyde in water.[11−13] The Lewis acid sites of these oxides are considered to be unsaturated coordination species, such as tetrahedrally coordinated niobium and titanium species on the surface.[11,12] In this study, we have focused on Lewis acid catalysis of TiO_4-deposited mesoporous silica (TDMS). It has been reported that the introduction of titanium species onto the silica surface would preferentially result in the formation of TiO_4 tetrahedra,[14−17] but the Lewis acid catalysis for such species in water has not yet been studied. Here, we report that

Received: December 5, 2013
Revised: February 19, 2014
Published: March 11, 2014

   dx.doi.org/10.1021/cs401149n | ACS Catal. 2014, 4, 1198−1204

isolated TiO_4 tetrahedra dispersed on mesoporous silica exhibit high catalytic performance that is distinct from that of TiO_2.

2. EXPERIMENTAL SECTION

2.1. Catalyst Preparation. Mesoporous silica SBA-15 was synthesized with an amphiphilic block copolymer P123 (Aldrich, M_W = 5800) as a structure-directing agent and tetramethyl orthosilicate (TMOS) as a silica source.[18,19] In a typical synthesis, 4 g of P123 was dissolved in a mixed solution of distilled water (90 g) and HCl (4 M, 60 mL) at 313 K. After addition of TMOS (6.2 g) into the clear solution, the mixture was stirred at 313 K for 20 h, followed by heating at 373 K for 24 h under static conditions. Calcination of the resultant white precipitate at 823 K for 5 h in air resulted in mesoporous silica SBA-15.

Impregnation of titanium species onto SBA-15 was performed by a simple postgrafting method.[15] SBA-15 (5 g) was added to a mixture of distilled water (145 g) and ethanol (15 g) at room temperature. After the pH of the solution was adjusted to 10.0 with diluted ammonia, a mixture of ethanol (5 g), Ti(*i*-pro)$_4$ (TTIP), and acetyl acetone (AA) (AA/TTIP = 3.1) was slowly added to the mixture at 278 K and then stirred for 2 h. After filtration and repeated washing with ethanol, the material was calcined at 823 K for 3 h to immobilize the titanium species on the silica surface. The resulting TiO_4-deposited mesoporous silica (TDMS) samples with various titanium content are denoted as Ti-x/SBA-15 (x = Ti atom %).

For comparison, bulk anatase TiO_2 and titanosilicate zeolite (TS-1) were used as reference catalysts. TiO_2 was synthesized by a sol–gel method using Ti(*i*-pro)$_4$ as a precursor.[12] TS-1 was supplied from the Catalysis Society of Japan and was used as received.

2.2. Catalyst Characterization. The titanium content of the samples was determined using X-ray fluorescence spectroscopy (XRF; ZSX100e, Rigaku). Powder X-ray diffraction patterns were obtained with a diffractometer (Ultima IV, Rigaku) using Cu Kα radiation (40 kV, 40 mA) over the 2θ range of 0.7–70°. Nitrogen adsorption–desorption isotherms were measured at 77 K with a surface area analyzer (Nova-4200e, Quantachrome). Prior to measurement, the samples were heated at 473 K for 1 h under vacuum to remove physisorbed water. The Brunauer–Emmett–Teller (BET) surface areas were estimated over a relative pressure (P/P_0) range of 0.05–0.30. Pore size distributions were obtained from the adsorption branch of the isotherms using the Barrett–Joyner–Halenda (BJH) method. X-ray absorption spectra at the Ti–K edge were acquired at BL-9C of the Photon Factory of the Institute for Material Structure Science (PF-IMSS, KEK, proposal no. 2012G101). TS-1 and TDMS were pressed into 20 mm diameter self-supporting disks, and TiO_2 was pressed with boron nitride into a 20 mm diameter disk. Dehydrated samples were sealed in polyethylene bags under a nitrogen atmosphere. Data reduction was performed using the REX2000 program (Rigaku). The acid site density of the samples was estimated by Hammett indicator titration based on the Benesi method in dry benzene.[20,21] *n*-Butylamine and 4-phenylazo-1-naphthylamine (p*K*a = +4.0) were used as titrant and color indicator, respectively.

Fourier transform-infrared (FT-IR) spectra were obtained at a resolution of 4 cm^{-1} using a spectrometer (FT/IR-6100, Jasco) equipped with an extended KBr beam splitting device and a mercury cadmium telluride (MCT) detector. A total of 32 scans were averaged for each spectrum. The samples were pressed into self-supporting disks (20 mm diameter, 20 mg) and placed in an IR cell attached to a closed glass-circulation system. The disks were dehydrated by heating at 573 K for 1 h under vacuum to remove physisorbed water. For experiments with hydrated samples, the dehydrated disks were exposed to 20 Torr of water vapor at room temperature for 1 h, followed by evacuation for 5 min to remove weakly adsorbed water. CO was adsorbed as a basic probe molecule on the dehydrated or hydrated sample disks in the IR cell under cooling with liquid N_2 (measured temperature, 100 K). Each IR spectrum was measured after adsorbed CO and CO in the gas phase reached equilibrium. IR spectra of the samples measured at 100 K before CO adsorption were used as backgrounds for difference spectra by subtraction from the spectra measured for the CO-adsorbed samples.

2.3. Catalytic Reactions. Lewis acid catalysis of the prepared mesoporous titanosilicates was examined by the hydride transfer of pyruvaldehyde to lactic acid and the Mukaiyama-aldol condensation benzaldehyde with 1-trimethylsilyloxy-cyclohexene in water. In the typical hydride transfer reaction, a mixture of pyruvaldehyde solution (2 mL, 0.1 M) and catalyst (0.1 g) was heated in a sealed Pyrex glass vial at 383 K for 2 h. The solution was analyzed after reaction using high-performance liquid chromatography (HPLC; LC-2000 plus, Jasco) with a refractive index detector. For the Mukaiyama-aldol condensation, a mixture of benzaldehyde (0.4 mmol), 1-trimethysilyloxy-cyclohexene (0.6 mmol), sodium dodecyl sulfate (0.08 mmol), water (3 mL), and catalyst (100 mg) was stirred at 298 K for 2 h. The product isolated by solvent extraction with ethyl acetate was analyzed using ^{1}H nuclear magnetic resonance spectroscopy (NMR; Biospin AvanceIII 400 MHz, Bruker). Dioxane was used as an internal standard.

3. RESULTS AND DISCUSSION

3.1. Structure of TDMS. The mesoporous structure and mesoporosity of the samples were examined by X-ray diffraction (XRD) measurement and N_2 adsorption analysis, and the results are shown in Figures 1 and 2. All samples, including bare SBA-15, have well-defined XRD peaks at 0.9, 1.5, and 1.8° in Figure 1A. These peaks are assignable to (100), (110), and (200) diffraction of the two-dimensional hexagonal

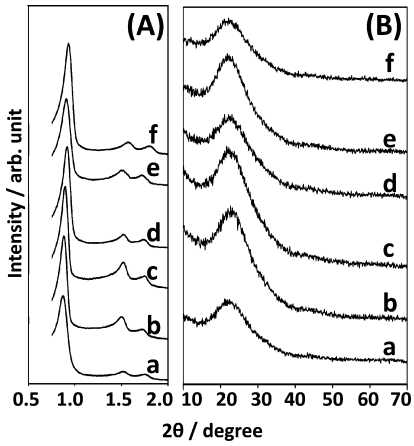

Figure 1. (A) Low-angle and (B) wide-angle XRD patterns for (a) bare SBA-15, (b) Ti-0.1/SBA-15, (c) Ti-0.25/SBA-15, (d) Ti-0.5/SBA-15, (e) Ti-1/SBA-15, and (f) Ti-2/SBA-15.

dx.doi.org/10.1021/cs401149n | *ACS Catal.* 2014, 4, 1198–1204

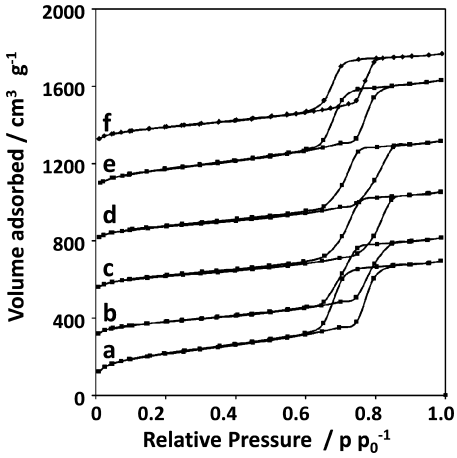

Figure 2. N_2 adsorption−desorption isotherms for (a) SBA-15, (b) Ti-0.1/SBA-15, (c) Ti-0.25/SBA-15, (d) Ti-0.5/SBA-15, (e) Ti-1/SBA-15, and (f) Ti-2/SBA-15. Each isotherm is vertically offset with 250 $cm^3\ g^{-1}$.

(*P6mm* symmetry of mesopores.[18,19] The lack of clear diffractions in the wide-angle range suggests that the titanium species are highly dispersed onto the mesoporous surface, even after calcination at 823 K (Figure 1B). The samples have a typical type-IV N_2 adsorption−desorption isotherm with an H1-type hysteresis loop that is characteristic of a mesoporous solid with uniform and large mesopores (Figure 2).[18,19] Table 1 summarizes the physicochemical properties of the samples. Although there is a slight decrease in the BET surface area and pore volumes of SBA-15 after immobilization of the titanium species, the samples still have large BET surface areas (432−483 $m^2\ g^{-1}$), pore volumes (0.74−0.80 mL g^{-1}), and uniform mesopores (ca. 9 nm) that are beneficial for catalytic applications. The titanium content of the samples increases continuously with the initial Ti(*i*-pro)$_4$ concentration and reaches 0.35 mmol g^{-1} for Ti-2/SBA-15.

The coordination environment of the titanium species was evaluated using UV−vis diffusive reflectance spectroscopy (UV−vis DRS) and X-ray absorption near edge structure (XANES) of the Ti K-edge. Figure 3 shows UV−vis DRS spectra for bare SBA-15 and the TDMS samples, in addition to that for a titanosilicate zeolite (TS-1) for comparison. SBA-15 shows no absorption band in the UV region; however, TS-1 and TDMS have an intense and narrow absorption band at 200−250 nm, which is assignable to the charge transfer of isolated TiO_4 tetrahedra.[14−17,22,23] It has been reported that TiO_4 tetrahedra in zeolite are stabilized by coordination of two H_2O molecules, forming octahedrally coordinated Ti species, $TiO_4(H_2O)_2$.[24,25] This suggests that octahedrally coordinated Ti species such as $TiO_4(H_2O)_2$ are also formed on TDMS in

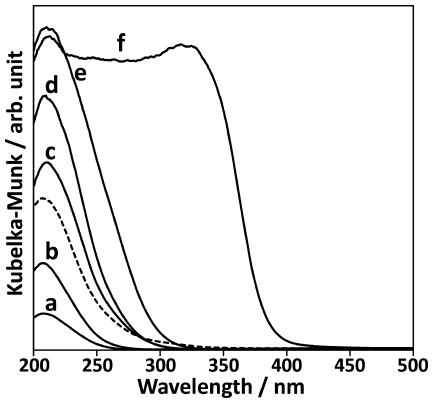

Figure 3. UV−vis DRS spectra of TDMS with various titanium content, TS-1 and anatase TiO_2. (a) Ti-0.1/SBA-15, (b) Ti-0.25/SBA-15, (c) Ti-0.5/SBA-15, (d) Ti-1/SBA-15, (e) Ti-2/SBA-15, and (f) anatase TiO_2. The spectrum for TS-1 is given as a dashed line.

the presence of water. The band intensity and absorption edge of the TiO_4 tetrahedra for TDMS increases and shifts to a longer wavelength with increasing introduced titanium content, and the band edge reaches ca. 300 nm for Ti-2/SBA-15. This can be attributed to the formation of TiO_6 octahedra: the adsorption band of TiO_6 octahedra appears at longer wavelength than that of TiO_4 tetrahedra. The absence of a strong and wide absorption band up to ca. 400 nm for anatase TiO_2 (Figure 3f) indicates that TDMS has no bulk TiO_2 particles. The formation of TiO_4 tetrahedra is also supported by XANES measurement. Figure 4 shows Ti K-edge XANES

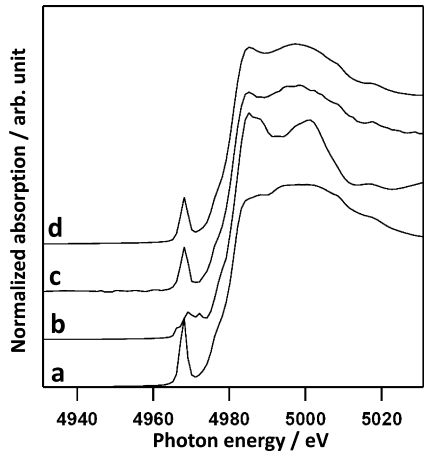

Figure 4. Ti K-edge XANES spectra for (a) TS-1, (b) TiO_2, (c) Ti-0.5/SBA-15, and (d) Ti-2/SBA-15.

Table 1. Physicochemical Properties of TDMS Samples

catalyst	S_{BET} ($m^2\ g^{-1}$)	pore diameter ($cm^2\ g^{-1}$)	pore volume (nm)	Ti content[a] (mmol g^{-1})	surface Ti density (nm^{-2})	Lewis acid site density[b] (mmol g^{-1})
SBA-15	742	0.90	9.3			
Ti-0.1/SBA-15	455	0.80	9.2	0.020	0.03	0.01[b]
Ti-0.25/SBA-15	429	0.78	9.4	0.049	0.07	0.02[b]
Ti-0.5/SBA-15	432	0.80	9.3	0.085	0.12	0.03[b]
Ti-1/SBA-15	483	0.77	9.4	0.170	0.21	0.11[b]
Ti-2/SBA-15	481	0.74	9.4	0.353	0.44	0.16[b]

[a]Determined from XRF measurements. [b]Hammett indicator titration based on the Benesi method.

dx.doi.org/10.1021/cs401149n | *ACS Catal.* 2014, 4, 1198−1204

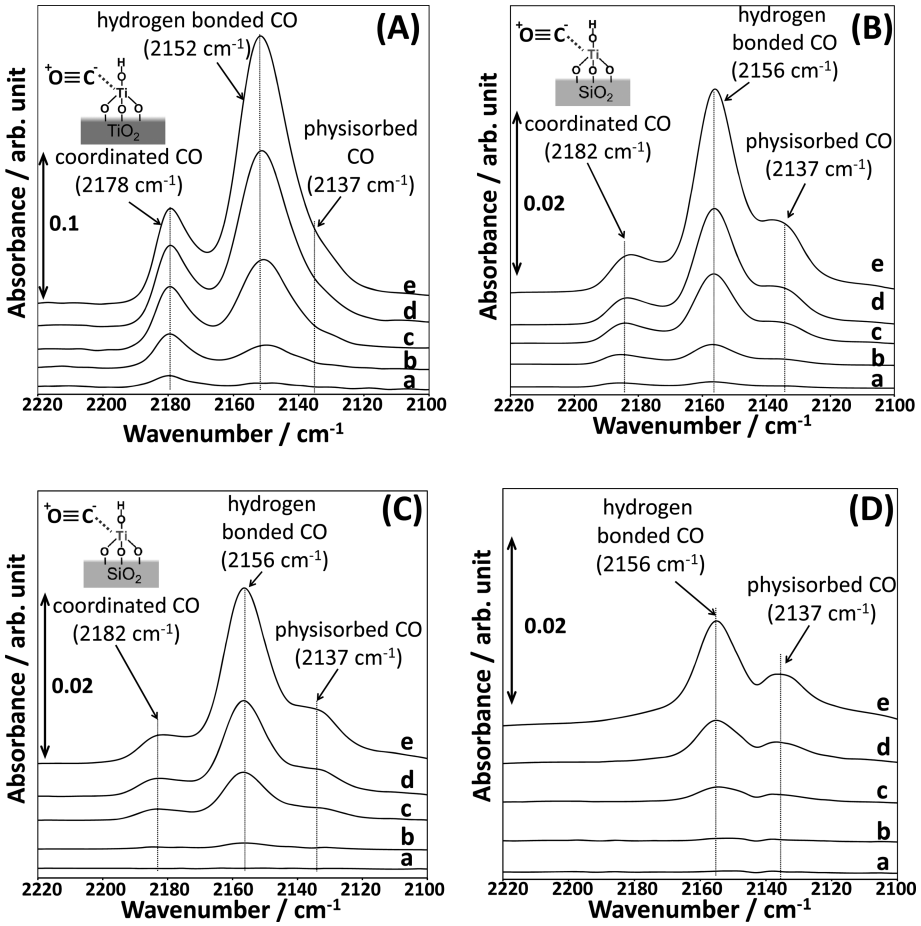

Figure 5. FT-IR difference spectra of CO-adsorbed (A) hydrated TiO_2, (B) dehydrated Ti-2/SBA-15, (C) hydrated Ti-2/SBA-15, and (D) dehydrated SBA-15 at 100 K. CO pressures for spectra a, b, c, d, and e correspond to 0.1, 0.2, 0.5, 1.0, and 2.0 Torr, respectively.

spectra of Ti-0.5/SBA-15, Ti-2/SBA-15, TS-1, and anatase TiO_2. TDMS has a similar pre-edge peak to that of TS-1, where a sharp pre-edge peak appears at around 4967 eV, which is attributed to the transition from the Ti 1s to Ti 3d mixed with O 2p of tetrahedrally coordinated titanium species.[24,26,27] In contrast, anatase TiO_2 shows typical weak pre-edge peaks assignable to the transition of octahedrally coordinated titanium centers. The UV−vis DRS results are compatible with the XANES spectra in terms of the formation of isolated TiO_4 tetrahedra on the mesopore surfaces. It was estimated from the XANES spectra for TS-1 and anatase TiO_2 that about half of the introduced titanium species are deposited as TiO_4 tetrahedra on SBA-15 in Ti-0.5/SBA-15 and Ti-2/SBA-15.

3.2. Lewis Acid Property and Catalysis of TDMS. Lewis acid site density for TDMS samples was also examined by Hammett indicator titration based on the Benesi method (Table 1). The density clearly increases with an increase in introduced titanium species and reaches 0.16 mmol g^{-1} for Ti-2/SBA-15. Table 1 also shows that 40−60% of introduced titanium species function as Lewis acid sites on all prepared TDMS samples: half of the introduced Ti species show no Lewis acidity. This is in good agreement with the results of XANES. In UV−vis DRS measurement, the absorption band edge of the TiO_4 tetrahedra for TDMS shifts to longer wavelength with increasing introduced titanium content, suggesting the formation of TiO_6 octahedra even at low Ti content. As a result, both unsaturated coordination TiO_4 tetrahedra and saturated coordination TiO_6 octahedra would be formed even at low Ti $(i\text{-pro})_4$ concentration.

The Lewis acid properties of the samples were investigated using FT-IR measurements with CO as a basic probe molecule (Figure 5). Figure 5A shows difference FT-IR spectra for CO-adsorbed hydrated anatase TiO_2. The intensities of the three bands at 2137, 2152, and 2178 cm^{-1} that are assigned to physisorbed CO, hydrogen-bonded CO with surface Ti−OH group,[28] and CO adsorbed on Lewis acid sites, respectively, increase with the amount of introduced CO. Therefore, anatase TiO_2 has Lewis acid sites that are active in the presence of water, which is in good agreement with the previous report.[12] Figure 5B,C show FT-IR spectra for CO-adsorbed dehydrated and hydrated Ti-2/SBA-15. Ti-2/SBA-15 also has three intense bands at 2137, 2156, and 2182 cm^{-1}, due to physisorbed CO, hydrogen-bonded CO with surface Si−OH group, and coordinated CO on Lewis acid sites, respectively, even in the presence of physisorbed water. This band for coordinated CO on Lewis acid sites is not observed for bare SBA-15 (Figure 5D): the bands at 2137 and 2156 cm^{-1} are derived from physisorbed CO and hydrogen-bonded CO with surface Si−OH group, respectively.[29−31] Thus, Lewis acid sites on TDMS samples can work even in the presence of water. Considering that TiO_4 tetrahedra on TDMS exist as octahedrally coordinated $TiO_4(H_2O)_2$ in the presence of water molecules, it is expected that coordinated H_2O molecules of the Lewis acid sites are replaced by CO, due to weak H_2O-Lewis acid interaction. It should be noted that the band position for

dx.doi.org/10.1021/cs401149n | ACS Catal. 2014, 4, 1198−1204

coordinated CO on hydrated Ti-2/SBA-15 (2182 cm^{-1}) is somewhat higher than that of hydrated anatase TiO_2 (2178 cm^{-1}), which suggests that there is a difference in acid strength between hydrated Ti-2/SBA-15 and anatase TiO_2.

Lewis acid catalysis with TDMS was examined through the hydride transfer of pyruvaldehyde to lactic acid and the Mukaiyama-aldol condensation of benzaldehyde with 1-trimethylsilyloxy-cyclohexene. Pyruvaldehyde is present in water as the original aldehyde, monohydrate, and dihydrate forms with typical equilibrium distributions of trace level, 57%, and 43%, respectively.[32] Monohydrate pyruvaldehyde can be converted into lactic acid on a water-tolerant Lewis acid catalyst through the intramolecular Meerwein–Ponndorf–Verley (MPV) mechanism (Table 2).[13] Table 2 shows the catalytic

Table 2. Catalytic Activities of the Samples and Reference Catalysts for the Hydride Transfer of Pyruvaldehyde to Lactic Acid in Water

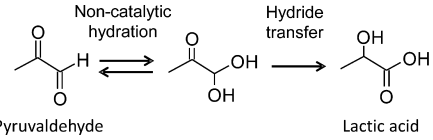

catalyst	Lewis acid site density (mmol g^{-1})	conversion (%)	yield (%)	selectivity (%)
H_2SO_4		16	2	13
$Sc(OTf)_3$	2.0	100	94	94
TiO_2	0.26[a]	100	49	49
TS-1	0.36[b]	95	82	86
SBA-15		29	0	
Ti-0.1/SBA-15	0.01[b]	51	45	88
Ti-0.25/SBA-15	0.02[b]	74	68	92
Ti-0.5/SBA-15	0.03[b]	86	80	92
Ti-1/SBA-15	0.11[b]	92	89	97
Ti-2/SBA-15	0.16[b]	91	90	98

Reagents and conditions: pyruvaldehyde, 0.2 mmol; catalyst, 100 mg; water, 2 mL; temperature, 383 K; time, 2 h. [a]FT-IR measurement using pyridine as a basic probe molecule. [b]Hammett indicator titration based on the Benesi method.

activities of the samples and reference catalysts for this reaction. H_2SO_4 as a Brønsted acid is not effective for the reaction;[13] however, scandium(III) triflate ($Sc(OTf)_3$),[33−35] a highly active and soluble water-tolerant Lewis acid catalyst, gave a high yield (94%) of lactic acid.[13] Therefore, $Sc(OTf)_3$ functions as an effective catalyst to promote hydride transfer in water. It has been reported that TiO_4 tetrahedra on anatase TiO_2 can function as water-tolerant Lewis acid sites in water, and anatase TiO_2 showed 100% conversion and 49% lactic acid yield.[12] The low lactic acid selectivity is due to simultaneous side reactions that proceed on the TiO_2 surface. The high lactic acid yield (82%) for TS-1 indicates that TiO_4 tetrahedra can act as active and selective sites for hydride transfer in water. Table 2 indicates that bare SBA-15 does not catalyze the reaction at all and that TDMS effectively catalyzes the reaction as well as TS-1; the pyruvaldehyde conversion and lactic acid yield for TDMS samples increase with the amount of Lewis acid sites and reached 90% yield over Ti-2/SBA-15. Table 3 summarizes the turnover frequency (TOF) for each catalyst at a pyruvaldehyde conversion of ca. 50%. While the Lewis acid sites on TiO_2 have the largest TOF on the basis of the pyruvaldehyde conversion, these are quite inferior to those of other catalysts with lactic

Table 3. TOF Values for Hydride Transfer Conversion of Pyruvaldehyde to Lactic Acid in Water

catalyst	Lewis acid site density (mmol g^{-1})	catalyst weight (g)	reaction time (min)	conversion (%)	TOF (h^{-1})
$Sc(OTf)_3$	2.0	0.05	5	47	11
TiO_2	0.26[a]	0.05	5	53	98
TS-1	0.36[b]	0.05	15	57	25
Ti-0.1/SBA-15	0.01[b]	0.1	120	51	51
Ti-0.25/SBA-15	0.02[b]	0.1	60	43	43
Ti-0.5/SBA-15	0.03[b]	0.1	30	46	61
Ti-1/SBA-15	0.11[b]	0.1	30	50	18
Ti-2/SBA-15	0.16[b]	0.1	30	45	11

Reagents and conditions: pyruvaldehyde, 0.2 mmol; water, 2 mL; temperature, 383 K. [a]FT-IR measurement using pyridine as a basic probe molecule. [b]Hammett indicator titration based on the Benesi method.

acid selectivity. $Sc(OTf)_3$, TS-1, and TDMS (Ti > 0.5 atom %) exhibit high lactic acid selectivity and yield, and there is no large difference in lactic acid selectivity and yield shown in Table 2. However, Table 3 reveals that TOF for TDMS under optimal conditions (Ti-0.5/SBA-15) is more than 2 to 6 times higher than those of $Sc(OTf)_3$ and TS-1. This indicates that TiO_4 tetrahedra on TDMS are not only selective for the hydride transfer conversion of pyruvaldehyde but also more active than $Sc(OTf)_3$ and the TiO_4 tetrahedra of TS-1. TDMS samples were readily separated from the reaction mixture by simple decantation or filtration. No significant decrease in lactic acid yield was observed even after three reuses of the samples (Figure 6).

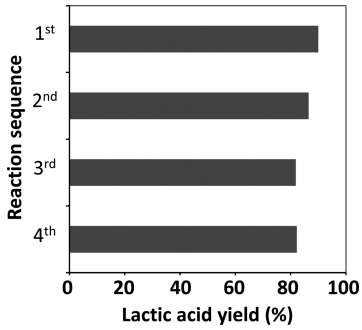

Figure 6. Catalyst reuse experiment using Ti-2/SBA-15 for the hydride transfer conversion of pyruvaldehyde to lactic acid in water at 383 K for 2 h.

TDMS was also evaluated by the Mukaiyama-aldol reaction of benzaldehyde with 1-trimethylsilyloxy-cyclohexene in water. It has been reported that the product yield of this reaction increases significantly in a water/tetrahydrofuran (THF) mixture or in a water–surfactant reaction system.[33−35] Water and sodium dodecyl sulfate (SDS) were adopted as a solvent and dispersing agent, respectively, for this study. Table 4 summarizes the acid site density, product yield, and turnover number (TON) of the samples and some reference catalysts. $Sc(OTf)_3$ exhibits a high product yield (82%), which is comparable to that for $Sc(OTf)_3$ in a water/THF reaction system.[33] TS-1 and anatase TiO_2 with TiO_4 tetrahedra Lewis acid sites do not work as effective catalysts for the Mukaiyama-aldol reaction. The difference in activity for the hydride transfer of pyruvaldehyde and the Mukaiyama-aldol reaction between

dx.doi.org/10.1021/cs401149n | ACS Catal. 2014, 4, 1198−1204

Table 4. Catalytic Activities of the Samples and Reference Catalysts for the Mukaiyama-Aldol Reaction of Benzaldehyde with 1-Trimethylsilyloxy-cyclohexene in Water

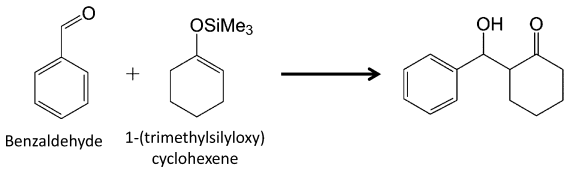

catalyst	Lewis acid site density (mmol g^{-1})	yield[a] (%)	TON
$Sc(OTf)_3$	2.0	82	1.6
TiO_2	0.26[b]	3	0.5
TS-1	0.36[c]	9	1.0
SBA-15		2	
Ti-0.1/SBA-15	0.01[c]	17	68
Ti-0.5/SBA-15	0.03[c]	67	89
Ti-2/SBA-15	0.16[c]	93	23

Reagents and conditions: benzaldehyde, 0.4 mmol; 1-trimethylsilyloxy-cyclohexene, 0.6 mmol; SDS, 0.08 mmol; water, 3 mL; catalyst, 100 mg; temperature, 298 K; time, 2 h. [a]Syn/anti ratio for all tested catalysts was estimated to be ca. 7/3. [b]Determined by pyridine-adsorption experiment using FT-IR. [c]Determined by Hammett indicator titration based on the Benesi method.

TS-1 and TDMS might be due to microporous structure. The micropores of TS-1 can prevent diffusion of reactants and products, limiting the catalysis of a high density of TiO_4 tetrahedra in TS-1. In contrast to TS-1 and TiO_2, the TDMS samples have product yields comparable to that of $Sc(OTf)_3$ and TON that are larger than that of $Sc(OTf)_3$. Tables 3 and 4 also show that Ti-0.5/SBA-15 exhibits the highest TOF for the hydride transfer of pyruvaldehyde into lactic acid and the largest TON for the Mukaiyama-aldol reaction. However, Ti-2/SBA-15 that has a higher Lewis acid density than Ti-0.5/SBA-15 is inferior to Ti-0.5/SBA-15 in TOF and TON for both reactions, indicating that the Lewis acid sites of the former have lower reactivity than those of the latter. The absorption band intensity and absorption edge of the TiO_4 tetrahedra for TDMS increases and shifts to longer wavelength with increasing introduced titanium content as shown in UV–vis DRS for TDMS (Figure 3). This is due to the formation of TiO_6 octahedra that has an absorption band at longer wavelength than that of TiO_4 tetrahedra. An increase in TiO_6 species or aggregation of TiO_6 species might decrease the activity of Lewis acid sites on TDMS.

To summarize, TDMS exhibits higher catalytic performance for the tested Lewis acid catalyzed reactions in the presence of water than TiO_2 and TS-1: the catalytic activity of TDMS is comparable to that of $Sc(OTf)_3$, a highly active homogeneous Lewis acid catalyst. Such high catalytic performance of solid acid catalysts has been often attributed to either porous structure or acid strength, or both.[36,37] While mesoporous structure may facilitate diffusion and access of reactant molecules to the active sites, poor catalytic activity of TiO_2 for the Mukaiyama-aldol reaction cannot be explained solely by mesoporous structure. It should be noted that in the presence of water, the IR band for CO-adsorbed Lewis acid sites on TDMS is observed at higher wavenumber (2182 cm^{-1}) than that of TiO_2 (2178 cm^{-1}) in the CO adsorption experiment (Figure 5). This is due to the replacement of H_2O with CO on Ti species such as octahedral coordination $TiO_4(H_2O)_2$ in zeolites and suggests that there is a difference in reactivity or H_2O–CO replacement capability between Lewis acid sites of TDMS and TiO_2. One possible explanation for the difference is an essential distinction in TiO_4 Lewis acid sites between both materials. The Lewis acid sites on TiO_2 are regarded as Ti–O unsaturated coordination spheres, and positive charges in the Lewis acid centers can be compensated by delocalized electrons throughout the conduction band based on the Ti3d orbital. On the other hand, it has been reported that in transition metal-exchanged zeolite, metal cations in an insulator, the positive charges of metal cations are compensated by negative charges localized on the framework, suggesting that such local charge separation also occurs on TDMS surface.[38] As a result, the Lewis acid sites of both materials are expected to differ in environment, electronic state, and this may cause the difference in catalysis between TDMS and TiO_2. The details are currently under investigation.

4. CONCLUSION

TDMS prepared by the postgrafting method was investigated as solid Lewis acid catalyst in water. FTIR measurement reveals that TiO_4 tetrahedra on mesoporous silica can interact with carbon monoxide even in the presence of water. The TiO_4 tetrahedra deposited on mesoporous silica exhibit Lewis acid catalysis distinct from that of TiO_4 tetrahedra on TiO_2, and they act as highly selective and active sites for the hydride transfer of pyruvaldehyde to lactic acid and the Mukaiyama-aldol condensation of benzaldehyde with 1-trimethylsilyloxy-cyclohexene.

AUTHOR INFORMATION

Corresponding Author

*E-mail: mhara@msl.titech.ac.jp.

Notes

The authors declare no competing financial interest.

ACKNOWLEDGMENTS

This work was partly supported by the Core Research for Evolutional Science and Technology (CREST, JY230195), program of the Japan Science and Technology (JST) Corporation, and by a Sasakawa Scientific Research Grant from The Japan Science Society.

REFERENCES

(1) Corma, A.; García, H. *Chem. Rev.* **2003**, *103*, 4307–4366.
(2) *Lewis Acid in Organic Synthesis*; Yamamoto, H., Ed.; Wiley-VCH: Weinheim, 2000.
(3) Anastas, P. T.; Kirchhoff, M. M. *Acc. Chem. Res.* **2002**, *35*, 686–694.
(4) Nagayama, S.; Kobayashi, S. *Angew. Chem., Int. Ed.* **2000**, *39*, 567–569.
(5) Gu, W.; Zhou, W.-J.; Gin, D. L. *Chem. Mater.* **2001**, *13*, 1949–1951.
(6) Corma, A.; Nemeth, L. T.; Renz, M.; Valencia, S. *Nature* **2001**, *412*, 423–425.
(7) Corma, A.; Fornés, V.; Iborra, S.; Mifsud, M.; Renz, M. *J. Catal.* **2004**, *221*, 67–76.
(8) Moliner, M.; Román-Leshkov, Y.; Davis, M. E. *Proc. Natl. Acad. Sci. U.S.A.* **2010**, *107*, 6164–6168.
(9) Román-Leshkov, Y.; Moliner, M.; Labinger, J. A.; Davis, M. E. *Angew. Chem., Int. Ed.* **2010**, *49*, 8954–8957.
(10) Pescarmona, P. P.; Janssen, K. P. F.; Delaet, C.; Stroobants, C.; Houthoofd, K.; Philippaerts, A.; De Jonghe, C.; Paul, J. S.; Jacobs, P. A.; Sels, B. F. *Green Chem.* **2010**, *12*, 1083–1089.

(11) Nakajima, K.; Baba, Y.; Noma, R.; Kitano, M.; Kondo, J. N.; Hayashi, S.; Hara. *J. Am. Chem. Soc.* **2011**, *133*, 4224−4227.
(12) Nakajima, K.; Noma, R.; Kitano, M.; Hara, M. *J. Phys. Chem. C.* **2013**, *117*, 16028−16033.
(13) Koito, Y.; Nakajima, K.; Kitano, M.; Hara, M. *Chem. Lett.* **2013**, *42*, 873−875.
(14) Bérubé, F.; Nohair, B.; Kleitz, F.; Kaliaguine, S. *Chem. Mater.* **2010**, *22*, 1988−2000.
(15) Kim, T.-W.; Kim, M.-J.; Kleitz, F.; Nair, M. M.; Guillet-Nicolas, R.; Jeong, K.-E.; Chae, H.-J.; Kim, C.-U.; Jeong, S.-Y. *ChemCatChem* **2012**, *4*, 687−697.
(16) Capel-Sanchez, M. C.; Blanco-Brieva, G.; Campos-Martin, J. M.; de Frutos, M. P.; Wen, W.; Rodriguez, J. A.; Fierro, J. L. G. *Langmuir* **2009**, *25*, 7148−7155.
(17) Wu, P.; Tatsumi, T.; Komatsu, T.; Yashima, T. *Chem. Mater.* **2002**, *14*, 1657−1664.
(18) Zhao, D.; Feng, J.; Huo, Q.; Melosh, N.; Fredrickson, G. H.; Chmelka, B. F.; Stucky, G. D. *Science* **1998**, *279*, 548−552.
(19) Zhao, D.; Sun, J.; Li, Q.; Stucky, G. D. *Chem. Mater.* **2000**, *12*, 275−279.
(20) Benesi, H. A. *J. Am. Chem. Soc.* **1956**, *78*, 5490−5494.
(21) Benesi, H. A. *J. Phys. Chem.* **1957**, *61*, 970−973.
(22) Capel-Sanchez, M. C.; de la Peña-O'Shea, V. A.; Campos-Martin, J. M.; Fierro, J. L. G. *Top. Catal.* **2006**, *41*, 27−34.
(23) Zecchina, A.; Spoto, G.; Bordiga, S.; Ferrero, A.; Petrini, G.; Leofanti, G.; Padovan, M. *Stud. Surf. Sci. Catal.* **1991**, *69*, 251−258.
(24) Bordiga, S.; Bonino, F.; Damin, A.; Lamberti, C. *Phys. Chem. Chem. Phys.* **2007**, *9*, 4854−4878.
(25) Bordiga, S.; Damin, A.; Bonino, F.; Ricchiardi, G.; Zecchina, A.; Tagliapietra, R.; Lamberti, C. *Phys. Chem. Chem. Phys.* **2003**, *5*, 4390−4393.
(26) Chen, S.-Y.; Tang, C.-Y.; Lee, J.-F.; Jang, L.-Y.; Tatsumi, T.; Cheng, S. *J. Mater. Chem.* **2011**, *21*, 2255−2265.
(27) Farges, F.; Brown, G. E.; Rehr, J. J. *Phys. Rev. B* **1997**, *56*, 1809−1819.
(28) Hadjiivanov, K. I.; Klissurski, D. G. *Chem. Soc. Rev.* **1996**, *25*, 61−69.
(29) Beebe, T. P.; Gelin, P.; Yates, J. T. *Surf. Sci.* **1984**, *148*, 526−550.
(30) Cairon, O.; Chevreau, T.; Lavalley, J.-C. *J. Chem. Soc., Faraday Trans.* **1998**, *94*, 3039−3047.
(31) Matsunaga, Y.; Yamazaki, H.; Yokoi, T.; Tatsumi, T.; Kondo, J. N. *J. Phys. Chem. C* **2013**, *117*, 14043−14050.
(32) Nemet, I.; Vikić-Topić, D.; Varga-Defterdarović, L. *Bioorg. Chem.* **2004**, *32*, 560−570.
(33) Kobayashi, S.; Hachiya, I. *J. Org. Chem.* **1994**, *59*, 3590−3596.
(34) Kobayashi, S.; Wakabayashi, T.; Nagayama, S.; Oyamada, H. *Tetrahedron Lett.* **1997**, *38*, 4559−4562.
(35) Kobayashi, S.; Nagayama, S.; Busujima, T. *J. Am. Chem. Soc.* **1998**, *120*, 8287−8288.
(36) Tagusagawa, C.; Takagaki, A.; Iguchi, A.; Takanabe, K.; Kondo, J. N.; Ebitani, K.; Tatsumi, T.; Domen, K. *Chem. Mater.* **2010**, *22*, 3072−3078.
(37) Rao, Y.; Trudeau, M.; Antonelli, D. *J. Am. Chem. Soc.* **2006**, *128*, 13996−13997.
(38) Schoonheydt, R.; Geerlings, P.; Pidko, E.; Santen, R. A. *J. Mater. Chem.* **2012**, *22*, 18705−18717.